Journal of Power Sources 182 (2008) 594–598

Contents lists available at ScienceDirect

Journal of Power Sources

journal homepage: www.elsevier.com/locate/jpowsour

Short communication

Studies of residual stresses in planar solid oxide fuel cells

J. Malzbender*, W. Fischer, R.W. Steinbrech

Research Center Jülich GmbH, Institute for Microstructure and Properties of Materials, 52425 Jülich, Germany

ARTICLE INFO

Article history:
Received 6 March 2008
Received in revised form 31 March 2008
Accepted 9 April 2008
Available online 22 April 2008

Keywords:
Solid oxide fuel cell
Yttria-stabilized zirconia
Brazing
Residual stress
X-ray diffraction
Thermo-elastic modelling

ABSTRACT

Planar solid oxide fuel cells (SOFCs) are composites consisting of porous and dense functional layers as electrodes and electrolyte, respectively. Due to the thermo-elastic mismatch between the individual layers residual stresses develop during manufacturing that result in warping for unconstrained cells. The residual stress of half-cells specimens with oxidized anode has been determined as a function of temperature. Two complementary techniques, X-ray diffraction analyses and measurements of cell curvature were applied. Moreover, changes in electrolyte residual stress associated with cell brazing to a steel interconnect were measured. The joining was carried out with symmetric cell composites having an anode layer sandwiched between two electrolyte layers. In addition to this test the effect of brazing and welding on the stress situation in the electrolyte of a real cell was tested.

1. Introduction

Today, with substantial advances in theoretical understanding and experimental realization, the solid oxide fuel cell (SOFC) is considered to be a highly efficient device to convert chemical fuels directly into electrical power. In particular, in the past decade SOFC development has made significant progress resulting in a tenfold increase of power density [1]. There are essentially two main concepts under development, the tubular and the planar design [2]. Concerning long-term stability and demonstration of plant technology, the tubular concept is far more advanced, whereas the planar design offers higher volumetric and gravimetric power density [1]. But the development of robust, mechanically reliable planar SOFC stacks with the complex multilayer composite arrangement of cells and interconnects still faces various problems. These are related to differences in high-temperature properties of the involved materials and their partial lack of thermo-chemical and thermo-mechanical compatibility in the stack composite [3].

The planar SOFC is a layered composite which consists basically of three layers, anode, electrolyte and cathode, where in actual cell designs either interfacial functional layers are added or gradients in material properties are tailored [4]. Since the layers are rigidly bonded, any mismatch in thermal expansion of the materials results in residual stresses which are reflected in the pronounced curvature of unconstrained cells. Additional stresses can also emanate from the final arrangement and fixation of the cells in the SOFC stack. Frequently rigid glass ceramic sealants are used for stationary designs [5,6] and metallic brazes for auxiliary power units (APU) in mobile applications [7,8]. Especially the operating conditions of an SOFC–APU generate high demands on materials, stack design and fabrication. Typical service temperatures of about 800 °C are currently favored for an economically efficient operation. But it is also desirable that power is provided within short time after the initialization. Thus the stack must be heatable as rapidly as possible, which implies that high thermal loads will act on the different components and joints.

Thermal gradients developing during thermal cycling [9] or isothermal operation as well as reduction and oxidation processes [10,11] are a major source of residual stresses. These stresses should not exceed the generally low, probability dependent fracture strength of the brittle SOFC materials [12,13]. Hence, whereas steady-state operation of SOFC stacks is associated with degradation due to chemical processes, thermal and re-oxidation cycling may lead to fracture of the sealant or the cell and thereby to fatal damage of the entire stack [10,14].

With respect to stress development in SOFC composites there are two aspects that have only received limited consideration to date. Although room temperature residual stresses in anode supported planar SOFCs have been reported [15–18], little information is available on their quantitative level at high temperature and in the constrained configuration of a stack. Particular interest is directed to anode supported, thin electrolyte SOFCs at elevated temperature and to the effect of the sealant on the residual stress

* Corresponding author. Tel.: +49 2461 61 6964; fax: +49 2461 61 3699.
E-mail address: j.malzbender@fz-juelich.de (J. Malzbender).

0378-7753/$ – see front matter © 2008 Elsevier B.V. All rights reserved.
doi:10.1016/j.jpowsour.2008.04.035

level of the cell. Hence, aiming at a better insight into the thermo-mechanics and associated failure processes of solid oxide fuel cells in a stack, residual stresses in the electrolyte have been determined as a function of temperature using X-ray diffraction (XRD) methods [19,20] and measurement of cell curvature [21]. Moreover, changes in residual stress associated with joining of cells and interconnect have been studied for symmetric cells brazed to a ferritic metal interconnect.

2. Experimental

2.1. Unconstrained cell

SOFC half-cells (without cathode) were used for the XRD studies of the residual stress between room temperature and 900 °C. The half-cells comprised an approximately 350-μm thick porous ZrO_2(8 mol% Y_2O_3)/NiO anode substrate, anode functional layer (AFL), and ~10-μm thick ZrO_2(8 mol% Y_2O_3) electrolyte. The AFL had the same composition as the substrate but higher density.

2.2. Joined cell

The brazing effect was studied for a symmetric cell composites consisting of a 1.5-mm thick porous ZrO_2(8 mol% Y_2O_3)/NiO anode substrate sandwiched between ~10-μm thick ZrO_2(8 mol% Y_2O_3) electrolyte layers. In this case the free surface of the additional electrolyte layer was used to probe the residual stress. The stress was measured in the initial state, after deposition of an AgCuTi braze [8] on one surface of the cell and after brazing the symmetric cell to a thin sheet (~200 μm) of the ferritic Crofer22APU interconnect material at approximately 1000 °C.

2.3. X-ray diffraction

In the XRD studies the standard $\sin^2\psi$ method in ψ-geometry and Cu–K radiation was employed for measurement of the lattice strain in the polycrystalline 8YSZ electrolyte. To get enough intensity for a local resolution of about 1 mm^2 a polycapillary semi-lens was mounted in the incident beam path. The parallel beam behind the semi-lens was collimated to 0.6 mm × 1 mm by crossed slits. X-ray elastic constants of Eigenmann et al. [22] were used for converting the measured strain value to stress. The stress was determined assuming a plane unidirectional stress field. Further experimental details are given in [15].

2.4. Curvature studies

In the case of the curvature measurements one side face of specimen strips (~40 mm × 10 mm × half-cell thickness) was polished to permit in situ observation of the cross-section. The curvature measurement was carried out in a resistance heated furnace. The experimental set-up consisted of a long distance optical microscope mounted on a *x*–*y* positioning stage [23]. The heating rate was 8 K/min. The curvature of the specimens was determined for each selected temperature measuring in cross-section orientation positions on the specimen contour. The *x*–*y* co-ordinates permitted a calculation of the radius of curvature via a spherical fit.

2.5. Residual stress in a joined cell

In addition to the stress analysis in brazing tests with smaller symmetric half-cell specimens reported above the effect of brazing and welding on the stress situation was also examined during the fabrication of the repeating stack units (cassettes). The stress was measured in the electrolyte of a real size cell (~145 mm × 85 mm × half-cell thickness) using the XRD analysis.

The first joining step for the real size cell in the so-called CS design [24,25] consisted in brazing the ceramic cell into a metallic frame (Fig. 5) which contains the holes for the supply and discharge of air and fuel gas.

Reactive air brazing (RAB) was selected for fixing and sealing the cells into the frame sheet. RAB is particularly suited since it can be applied under oxidizing conditions in air. Frequently used brazing techniques for metal–ceramic joints need, in contrast to RAB, reducing (vacuum) conditions. But reduced oxygen partial pressure is known to partially decompose the ceramic cathode. Experimentally, the cell and the frame sheet were positioned in a metallic jig and brazed at 1050 °C in a resistively heated furnace in air (atmosphere) under a dead weight, i.e. a load of approximately 10 kg.

In the next joining step of the cassette fabrication, the brazed cell frame unit is welded to a base sheet of Crofer22APU, see Fig. 5. This step also includes the insertion of spacer rings for guided air and fuel gas transport and the fixation of a nickel mesh on the base sheet to facilitate contacting with the anode substrate.

Micro-laser beam welding is applied (pulsed Nd:YAG laser) which has the advantage of inserting the required welding energy very precisely with a high power density. Hence also the thermally induced residual stresses are minimized which otherwise can distort the finished brazed joint and lead to permanent damage, e.g. the fracture of the ceramic cell.

The XRD measurements were carried out twice with a 1-mm *x*- and *y*-shift. Five characteristic positions, in the centre of the long and short side of the cell and near the edges were selected. Due to symmetry three characteristic positions resulted there from. The obtained experimental values were grouped as the average of the minimum, maximum and average of the average value for each characteristic position and compared to the initial values (min., max. and average) for the free cell.

To evaluate the residual stresses the materials elastic moduli are needed. The elastic modulus of the anode substrate (oxidized ~100 GPa, reduced ~40 GPa) and AgCuTi braze (~75 GPa) were obtained from depth sensitive indentation [26]. The material properties of the commercially available Crofer22APU steel were adopted from the manufacturer (ThyssenKrupp AG) data sheet.

3. Results and discussion

In the subsequent sections the residual stresses are presented as a function of temperature for an unconstrained cell, then the changes in residual stress associated with interconnect—cells joining are described and finally the influence of the cassette welding on the residual stress is addressed.

3.1. Residual stress of an unconstrained half-cell

The XRD study revealed that the dense ~10-μm thick YSZ electrolyte layer on an oxidized ~350-μm thick NiO/YSZ anode substrate is facing a RT compressive residual stress of about −600 MPa (Fig. 1). The high RT value of the compressive stress decreases smoothly with temperature, at 800 °C the electrolyte stress is approximately −50 MPa (Table 1), and becomes negligible at about 900 °C. The change of stress appears to decrease with increasing temperature.

Similarly, the curvature of half-cell strips decreases non-linearly with increasing temperature and diminishes at higher temperatures (Fig. 2). To correlate XRD results and curvature data the residual stress was calculated from the curvature in combination with the thicknesses and elastic modulus of the anode substrate.

Table 1
Residual stresses and associated strains

Cell and test condition	Electrolyte residual stress (MPa)	Thickness electrolyte (μm)	Thickness anode substrate (mm)	Strain (%)
Oxidized, RT	~−600	10	0.35	0.37
Oxidized, RT	~−560 [15]	10	1.5	0.29
Oxidized, RT	~−660 [16,17]	20–40	2	0.36–0.38
Oxidized, RT	~−400 [17]	20	300	0.31
Oxidized, RT	~−600 [18]	10	510	0.35
Oxidized, 800 °C	~−50	10	0.35	0.03
Oxidized, 800 °C	~−50 [17]	20	300	0.04
Oxidized, 800 °C	~−100 [18]	10	510	0.06
Reduced, RT	~−520 [15]	10	1.5	0.29
Reduced, RT	~−670 [16]	20–40	2	0.39–0.44
Reduced, RT	~−200 [17]	20	300	0.21
Reduced, RT	~−300 [18]	10	510	0.20
Reduced, 800 °C	~−50 [17]	20	300	0.05
Reduced, 800 °C	~−50 [18]	10	510	0.04

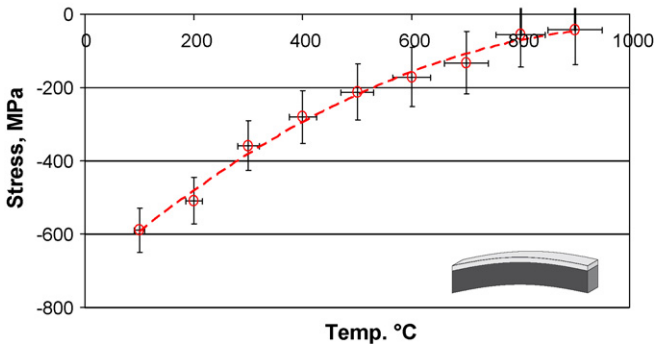

Fig. 1. Electrolyte stress (X-ray diffraction) (oxidized half-cell, anode ~350 μm, electrolyte ~8 μm). Stress decreases with increasing temperature and is close to zero at 900 °C.

Note that for the anode substrate the slight temperature dependence of the elastic modulus of ~10% up to 800 °C [12] was neglected in the calculation. As simplified relationship can be derived for a thin electrolyte layer on the basis of the equations given in [27]:

$$\Delta\sigma_E = \frac{d_A^3 E_A}{6 d_E (d_A + d_E)} \Delta \frac{1}{r} \quad (1)$$

where $\Delta\sigma_E$ is the change in electrolyte stress, d_A is the thickness of the anode substrate, d_E is the thickness of the electrolyte layer, E_A is the elastic modulus of the anode and $\Delta(1/r)$ is the change in curvature.

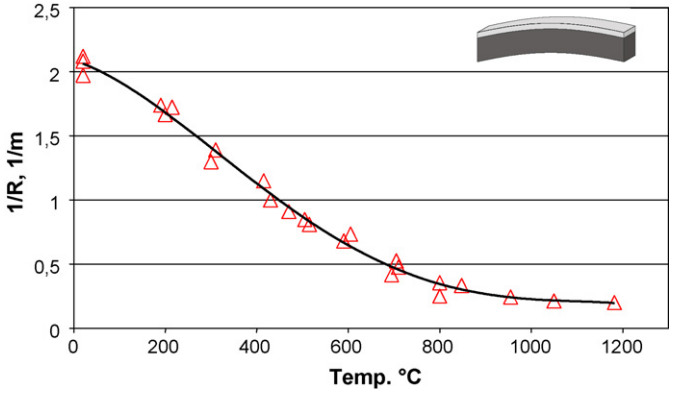

Fig. 2. Half-cell curvature (oxidized half-cell, anode ~350 μm, electrolyte ~8 μm). Curvature decreases with increasing temperature and is close to zero at ~900 °C.

A comparison of the residual stress in the electrolyte layer calculated using Eq. (1) and that determined using XRD in Fig. 3 shows good agreement of both methods. The RT values are also consistent with residual stress values published previously.

It has been shown previously that the overall room temperature XRD stress level in the electrolyte of a 1.5-mm thick cell was about −560 MPa for an oxidized anode substrate and −520 MPa for a reduced anode substrate [15]. Cells with slightly different anode geometry (2 mm) and electrolyte thickness (about 20–40 μm) led to a stress in the same order of magnitude of −660 ± 20 MPa for oxidized, flattened cells and −670 ± 10 MPa for reduced cells [16].

With respect to high-temperature diffraction studies on free cells only limited data are available from literature. Between RT and 800 °C a decrease from about −400 MPa to −50 MPa has been reported for 20-μm thick ScSZ electrolytes on 300-μm thick oxidized anodes and from −200 MPa to −50 MPa on reduced anodes [17]. Also a decrease from about −600 MPa to −100 MPa has been measured for 10-μm thick YSZ electrolytes on 510-μm thick oxidized anodes and from −300 MPa to −50 MPa for reduced anodes [18].

Hence, the room temperature values determined in the present work as well as the magnitude of the decrease of the compressive residual stress with increasing temperature are similar to these literature values. Note it has to be considered that differences in composition (ScSZ), thickness and porosity lead to a change of the actual stress values. The stress reported in [17] appears to decrease linear with increasing temperature, in [18] a non-linear decrease similar to our observations is reported.

Previous calculations of the high-temperature residual stress based on measured room temperature XRD studies and the average curvature change suggested fairly high electrolyte residual stress of more than −200 MPa at operation temperature (800 °C) [15]. The

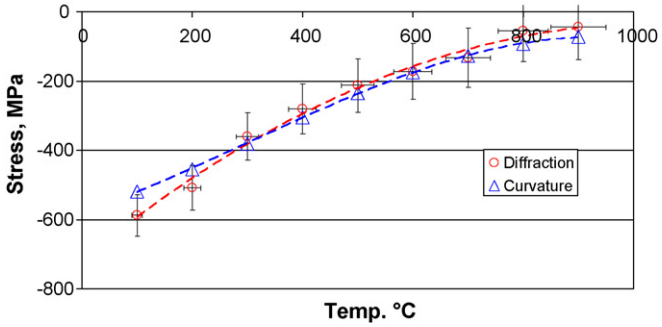

Fig. 3. Comparison of the experimentally determined residual stress with that calculated from the difference in thermal expansion coefficients.

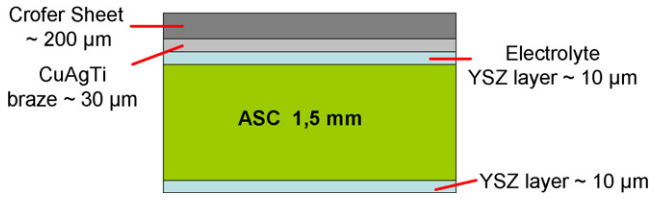

Fig. 4. Measurement of the stress in the YSZ layer opposite to the electrolyte. A symmetric composite was used since the stress in the free surface of the anode is too small to be assessed using X-ray diffraction. The application of an ASC with additional YSZ layer permits the determination of relatively small stress changes using a stress level shift.

deviation from the current result shows that non-linearity in curvature and hence difference in thermal expansion coefficient has a strong impact on the calculated residual stress.

The residual stresses also permit an estimate of the associated strain. Based on relationships in [27] a simplified solution for thin films can be derived:

$$\Delta\varepsilon = \frac{\Delta\sigma_E}{E_E} + 4\frac{\Delta\sigma_E t_E}{E_A t_A} \quad (2)$$

where $\Delta\varepsilon$ is the difference in strain, given by $\Delta\varepsilon = \int_{T_1}^{T_2} \Delta\alpha \cdot \Delta T$. Values of the strain for the electrolyte surface stresses determined here and reported in literature are listed in Table 1. The room temperature strain varies between 0.29 and 0.37% and the strain at 800 °C between 0.03 and 0.06% for cells with oxidized anode substrates. For cells with reduced anode substrates the variation is between 0.20 and 0.44% for the RT strain and 0.04 and 0.05% for the strain at 800 °C.

Although the determined compressive stress in the electrolyte is lower than the value of ~−200 MPa reported in a previous study [15], it appears still to be high enough to support mechanical robustness of the electrolyte layer. With this level of compressive residual stress a malfunction of a cell due to crack formation should not occur for an unconstrained cell. However, it should be noted that additional stresses can be imposed by mounting cells a SOFC stack.

Based on the electrolyte stresses also the residual stresses in the anode can be estimated [28]. The estimate leads to tensile stress values well below 10 MPa, which appears uncritical compared to typical anode fracture stresses in the order of 50–100 MPa. But note that if statistical aspects of the flaw size distribution are considered, cells can also fail at lower stress levels [29].

3.2. Residual stress of a joined cell specimen

The X-ray stress evaluation method was also applied to quantify the impact of reactive air brazing on the residual stress. In contrast to the electrolyte stress studies outlined before a symmetric cell composite was used to probe the residual stress at the free surface of the un-joined electrolyte layer (Fig. 4). The stress was measured in the initial state, after deposition of the Ag-based braze and after brazing the symmetric cell to a thin sheet of the ferritic interconnect material.

In the initial state the electrolyte layer used for the residual stress probing was under a compressive stress of approximately −570 MPa. After the braze was deposited at ~1000 °C on the electrolyte the stress increased by approximately −33 MPa (Table 2). After joining with braze the ferritic steel sheet to the symmetric cell the stress in the probing electrolyte increased by about −45 MPa compared to the initial state. Since the electrolyte layers were thin in comparison to the anode both possessed approximately the same strain. The stress induced in the anode is simply equal to the strain in the electrolyte layer times the ratio of anode to YSZ stiffness (~0.42), resulting in a value of ~−20 MPa. The average thermal

Table 2
Specimen geometry and electrolyte strain and stress for the brazing experiments

Electrolyte YSZ 10 μm ASC 1,5 mm YSZ layer 10 μm	Change in the YSZ layer opposite electrolyte	
	Strain	Stress
Braze ~ 30 μm	$\Delta\varepsilon = 0.015\%$	$\Delta\sigma = -33$ MPa
Crofer Sheet ~ 200 μm	$\Delta\varepsilon = 0.020\%$	$\Delta\sigma = -45$ MPa

expansion coefficient of the AgCuTi braze estimated from this stress change using the relationships given in [27] is ~$20 \cdot 10^{-6}$ K^{-1} suggesting a tensile stress in the brazing material of the order of 1 GPa. This stress is higher than the RT yield strength reported for the AgCuTi of approximately 300 MPa [30]. The high magnitude of the tensile stress requires future investigations with respect to defect formation, non-linear behavior and creep.

3.3. Residual stress of a joined cell

The stress was measured in five characteristic positions, in the centre of the long and short side of the cell and near the edges (Fig. 5). The measurement revealed that due to brazing the electrolyte residual stress in all positions changes by ~−3% being equivalent to −17 MPa. In the case of the welding the stress in the middle of the long side and near the edges alters by ~−4% (−22 MPa) whereas the stress in the middle of the short side changes by ~6% (32 MPa). The stress change in the anode substrate should be 50% lower due to its 50% lower stiffness, yielding a change of ~−9 MPa due to brazing and in the middle of the short side ~16 MPa due to welding. It has to be emphasised that this small effect should be uncritical.

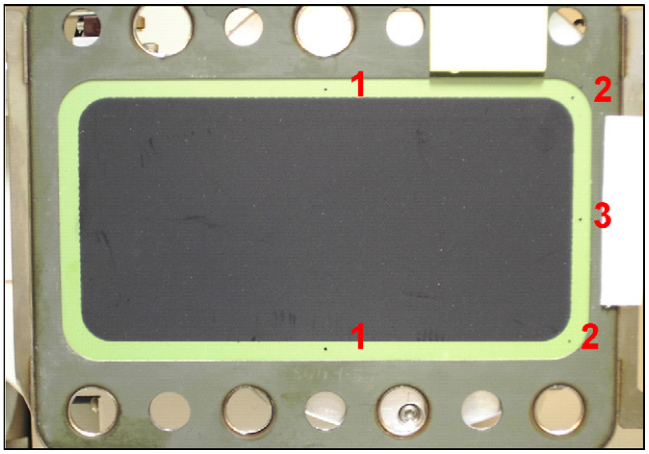

Fig. 5. Five characteristic positions for the evaluation of the brazing and welding effect on the residual stress of a real size cell in a cassette.

4. Conclusions

The present XRD studies have been carried out between room temperature and 900 °C in the dense electrolyte of half-cells. In the case of a ∼10-μm thick electrolyte layer on an oxidized ∼350-μm thick anode substrate the residual electrolyte stress takes a RT value of −600 MPa. The compressive stress decreases with temperature and becomes negligible at 900 °C. Similarly, the curvature of half-cell strips diminishes as a function of temperature. The electrolyte stress determined on the basis of the X-ray diffraction results correlates well with the stress calculated from the curvature data.

The X-ray stress evaluation methodology was also applied to analyze the impact of reactive air brazing on the residual stress. The effect was measured using a symmetric cell composites consisting of a thick anode sandwiched between ∼10-μm thick electrolyte layers. The un-joined electrolyte layer was used to probe the residual stress. The stress was measured in the initial state, after deposition of the Ag-based braze and after brazing of a thin sheet of the ferritic interconnect material. After joining the stress in the probing electrolyte had increased by about −45 MPa. The anode stress and the thermal expansion coefficient of the braze could be estimated from this stress change.

In addition to brazing a symmetric cell composite the effect of brazing and welding on the stress situation in the electrolyte of a real cell (∼85 mm × 145 mm) in the so-called CS design of the FZJ was tested. The XRD analysis of brazing and welding real size cells in cassettes revealed small changes of the residual stress. Change of ∼−9 MPa in the anode substrate due to brazing was lower than the ∼−20 MPa measured using a symmetric specimen. But the larger distance to the actual brazing trace need to be considered too. Cassette welding imposes in the middle of the short side only a small rather uncritical tensile stress change of ∼16 MPa.

Acknowledgements

The financial support of the German Federal Ministry of Economics and Technology (BMWi) is gratefully acknowledged (contract no. 0327703A). The authors would like to thank the members of the SOFC project at the FZJ, in particular J. Mertens for providing the SOFC material and A. Cramer and B. Kuhn for the specimen brazing and welding.

References

[1] L. Blum, W.A. Meulenberg, H. Nabielek, R. Steinberger-Wilckens, Int. J. Appl. Ceram. Technol. 2 (2005) 482.
[2] S.C. Singhal, Solid State Ionics 135 (2000) 305.
[3] O. Yamamoto, Electrochim. Acta 45 (2000) 2423.
[4] F. Tietz, H.-P. Buchkremer, D. Stöver, Solid State Ionics 152/153 (2002) 373.
[5] P. Batfalsky, V.A.C. Haanappel, J. Malzbender, N.H. Menzler, V. Shemet, I.C. Vinke, R.W. Steinbrech, J. Power Sources 155 (2006) 128.
[6] K.L. Ley, M. Krumpelt, R. Kumar, J.H. Meiser, J. Bloom, J. Mater. Res. 11 (1996) 1489.
[7] K.S. Weil, et al., J. Power Sources 152 (2005) 97.
[8] B. Kuhn, F.J. Wetzel, J. Malzbender, R.W. Steinbrech, L. Singheiser, Proceedings of the SOFC X, Electrochemical Society, 2007, p. 413.
[9] S.C. Singhal, K. Kendall, in: S.C. Singhal, K. Kendall (Eds.), High Temperature Solid Oxide Fuel Cells: Fundamentals, Design and Applications, Elsevier Ltd., Oxford, 2003, pp. 1–22.
[10] A. Atkinson, Solid State Ionics 95 (1997) 249.
[11] J. Malzbender, E. Wessel, R.W. Steinbrech, Solid State Ionics 176 (2005) 2201.
[12] J. Malzbender, R.W. Steinbrech, L. Singheiser, Ceram. Eng. Sci. Proc. 26/4 (2005) 293.
[13] J. Malzbender, R.W. Steinbrech, J. Eur. Ceram. Soc. 27 (2007) 2597.
[14] M. Ettler, G. Blass, N.H. Menzler, Proceedings of the Seventh European SOFC Forum, 2006, p. P0705.
[15] W. Fischer, J. Malzbender, G. Blass, R.W. Steinbrech, J. Power Sources 150 (2005) 73.
[16] H. Yakabe, Y. Baba, T. Sakurai, Y. Yoshitaka, J. Power Sources 135 (2003) 9.
[17] H. Sumi, K. Ukai, M. Yokoyama, Y. Mizutani, Y. Doi, S. Machiya, Y. Akinwa, K. Tanaka, Trans. ASME 3 (2006) 68.
[18] E. Lara-Curzio, Durability and reliability of solid oxide fuel cells solid state energy conversion alliance (SECA), Core Technology Peer Review Workshop, Tampa, FL (US), 01/27/2005–01/28/2005.
[19] V. Hauk, Structural and Residual Stress Analysis by Nondestructive Methods, Evaluation–Application–Assessment, Elsevier, 1997.
[20] V. Hauk, H. Hougardy, E. Macherauch, Conf. Residual Stresses, Darmstadt 1990, Deutsche Gesellschaft für Materialkunde - DGM Informationsgesellschaft mbH, Oberursel, 1991, pp. 3–20.
[21] J. Malzbender, T. Wakui, R.W. Steinbrech, L. Singheiser, Fuel Cell 2 (2006) 123.
[22] B. Eigenmann, B. Scholtes, E. Macherauch, Materialwiss. Werkst. 20 (1989) 314–325.
[23] J. Malzbender, T. Koppitz, S.M. Gross, R.W. Steinbrech, Proceedings of the Seventh European SOFC Forum, 2006, p. P0418.
[24] D. Federmann, W. Behr, A. Cramer, J. Remmel, U. Reisgen, S.M. Groß, W. Mertens, T. Koppitz, H. Ringel, K. Richter, Seventh European SOFC Forum, File No. P0425 (2006).
[25] A. Gubner, T. Nguyen-Xuan, M. Bram, J. Remmel, L.G.J. de Haart, Seventh European SOFC Forum, File No. B042 (2006).
[26] J. Malzbender, J.M.J. den Toonder, A.R. Balkenende, G. de With, Mater. Sci. Eng. 36 (2002) 47 (reports).
[27] J. Malzbender, R.W. Steinbrech, Surf. Coat. Technol. 176 (2004) 165.
[28] J. Malzbender, Appl. Phys. Lett. 84 (2004) 4661.
[29] J. Malzbender, R.W. Steinbrech, J. Euro. Ceram. Soc. 28 (2007) 247.
[30] K.S. Weil, J.Y. Kim, J.S. Hardy, Electrochem. Solid State Lett. 8 (2005) A133.